International Journal of Medicine
pISSN 1468-3814 | eISSN 2667-7008
https://theinternationalmedicine.com/

Original Researcher Article DOI: 10.61336/im/26-09-28

Spectrum And Mri Characteristics Of Osseous, Ligamentous And Soft-Tissue Wrist Abnormalities.

Dr. Manish Bhagat[1], Dr. Yash Yadav[2]*, Dr. Dinesh Yadav[3], Dr. Faraz Uddin Ansari[4].
[1]*Professor & Head of Department, Department of Radio-diagnosis., Sri Aurobindo Medical College & P.G. Institute, Indore.*
[2]*PG Resident, Department of Radio-diagnosis, Sri Aurobindo Medical College & P.G. Institute, Indore.*
[3]*ENT Specialist, District Hospital Ujjain*
[4]*PG Resident, Department of Radio-diagnosis, Sri Aurobindo Medical College & P.G. Institute, Indore.*

Correspondence:
Dr. Yash Yadav.
PG Resident, Department of Radio-diagnosis, Sri Aurobindo Medical College & P.G. Institute, Indore.

Received: 07-08-2026
Revised: 17-08-2026
Accepted: 29-08-2026
Published: 04-09-2026

Abstract

Background: Wrist injuries may involve multiple osseous and soft-tissue structures, making accurate assessment clinically challenging. MRI provides comprehensive evaluation of bone, marrow, ligaments, tendons, TFCC, synovium, and surrounding soft tissues. This study evaluated the frequency and patterns of Spectrum and MRI Characteristics of Osseous, Ligamentous and Soft-Tissue Wrist Abnormalities ***Methods:*** A hospital-based prospective cross-sectional analytical observational study was conducted in the Department of Radiodiagnosis, Sri Aurobindo Medical College and Postgraduate Institute, Indore, from June 2024 to November 2025. Patients presenting with wrist pain following trauma and referred for MRI were evaluated. Demographic and clinical characteristics, MRI findings, and available histopathological, FNAC, or intra-operative findings were recorded. MRI abnormalities were systematically categorized according to the anatomical structures involved. ***Results:*** Twenty-five patients were included in the final analysis. Males constituted 60.0% of the study population, while 72.0% were aged >30 years. Wrist pain was the most common presenting complaint (52.0%), and 60.0% had no history of trauma. Scaphoid fracture was the most frequent MRI finding (24.0%), followed by TFCC tear (16.0%), ganglion cyst (12.0%), infectious arthritis (12.0%), and scaphoid AVN (8.0%). Among scaphoid fractures, waist involvement was predominant (83.3%), while Herbert type B1 was the commonest pattern (50.0%). TFCC tears were predominantly central (75.0%) and degenerative (75.0%). MRI demonstrated excellent correlation with available reference findings, with most diagnostic categories showing 100% sensitivity, specificity, PPV, NPV, accuracy, Kappa, and AUC. ***Conclusion:*** MRI demonstrated a broad spectrum of wrist abnormalities and provided detailed characterization of associated structural involvement. Its excellent diagnostic concordance supports its role as a comprehensive and reliable modality for evaluation of clinically suspected wrist injuries.

Keywords: Wrist injury; Magnetic resonance imaging; MRI; Scaphoid fracture; TFCC tear; Ganglion cyst; Wrist pathology.

INTRODUCTION

Wrist injuries are common clinical presentations encountered in orthopedic, trauma, sports medicine, and radiology practice. The wrist is a complex anatomical region comprising multiple small carpal bones, intrinsic and extrinsic ligaments, tendons, cartilage, neurovascular structures, and synovial spaces. Because of this intricate anatomy, traumatic injuries may involve more than one structure simultaneously, and the complete extent of injury can be difficult to establish on clinical examination alone. Accurate imaging is therefore essential for diagnosis, treatment planning, and prevention of long-term functional impairment [1,2].

The wrist includes the radiocarpal, midcarpal, and distal radioulnar joints, with the triangular fibrocartilage complex (TFCC) playing an important role in distal radioulnar stability and load transmission. Trauma may result in fractures, ligamentous injuries, TFCC tears, tendon injuries, bone marrow abnormalities, or combinations of these lesions. Unrecognized or inadequately treated ligamentous injuries and associated fractures may lead to chronic pain, carpal instability, degenerative changes, and impaired wrist function [3,4]. Combined injuries are particularly important because the presence of multiple abnormalities may alter clinical management and surgical decision-making.

Conventional radiography remains the initial imaging modality for suspected wrist trauma and is useful for detecting obvious fractures and bony abnormalities. However, it has limited sensitivity for occult fractures, bone marrow edema, ligamentous injuries, tendon pathology, and other soft-tissue abnormalities. Computed tomography provides excellent visualization of cortical bone and complex fractures but has limited soft-tissue contrast and involves ionizing radiation. Ultrasonography is useful for dynamic assessment of superficia

l tendons and soft tissues but is operator-dependent and limited in evaluating deep intra-articular structures [7,8].
Magnetic resonance imaging (MRI) provides excellent soft-tissue contrast, multiplanar imaging, and comprehensive evaluation without ionizing radiation. It allows simultaneous assessment of bones, bone marrow, cartilage, ligaments, tendons, TFCC, synovium, nerves, and surrounding soft tissues, making it particularly valuable for detecting occult fractures and associated soft-tissue injuries [1,9]. MRI is highly sensitive for bone marrow edema and radiographically occult fractures and can demonstrate ligamentous injuries, including scapholunate, lunotriquetral, and TFCC abnormalities [10-12]. MR arthrography may further improve detection of subtle intra-articular ligamentous and TFCC tears when conventional MRI findings are inconclusive [13,14].

Given the complex anatomy and frequent coexistence of multiple traumatic abnormalities, systematic evaluation of MRI findings is important for identifying the Spectrum and MRI Characteristics of Wrist Abnormalities. The present study was therefore undertaken to evaluate the spectrum and combination patterns of Osseous, Ligamentous and Soft-Tissue Wrist Abnormalities detected on MRI, providing a comprehensive assessment that may assist in diagnosis, treatment planning, and prognostic evaluation.

MATERIALS AND METHODS

This hospital-based prospective cross-sectional analytical observational study was conducted in the Department of Radiodiagnosis, Sri Aurobindo Medical College and Postgraduate Institute (SAMC & PGI), Indore, Madhya Pradesh, India, over a period of 18 months from June 2024 to November 2025, following approval from the Institutional Ethics Committee.

Written informed consent was obtained from all participants or their legally authorized representatives before enrollment. Patient confidentiality was maintained using unique study identification numbers, and participation was voluntary without affecting routine clinical management. MRI examinations were performed as part of routine clinical care, and no additional intervention was undertaken solely for study participation.

Inclusion and Exclusion Criteria

A total of 25 patients of all age groups and either sex presenting with wrist pain following trauma and referred for MRI evaluation during the study period were enrolled using consecutive sampling. Patients were eligible if MRI of the wrist was clinically indicated, irrespective of whether subsequent surgical intervention was performed.
Patients who declined written informed consent and those unable to undergo MRI because of standard contraindications, including non-MRI-compatible implants, pacemakers, or severe claustrophobia, were excluded.

Methodology

Participants and Sampling

Following written informed consent, demographic characteristics, clinical history, mechanism of trauma, presenting complaints, clinical examination findings, provisional diagnosis, MRI findings, and available histopathological, FNAC, or intra-operative findings were recorded using a predesigned structured proforma. Consecutive sampling was used, and all eligible patients presenting during the study period were considered for enrollment.

MRI Examination and Image Analysis

All MRI examinations were performed using 1.5-Tesla and 3-Tesla Siemens Magnetom MRI systems with dedicated wrist or musculoskeletal surface coils. Imaging was performed using optimized wrist protocols with a small field of view and thin sections to achieve adequate spatial and contrast resolution.

The routine MRI protocol included two-dimensional fast spin-echo sequences and fluid-sensitive T2-weighted and proton-density sequences in three orthogonal planes. Coronal T1-weighted non-fat-suppressed sequences were obtained for assessment of carpal alignment, fracture lines, and bone marrow abnormalities. STIR sequences were used when chemical fat suppression was inadequate. Patients were positioned according to comfort and scanner requirements, with appropriate wrist alignment maintained to minimize motion and orientation-related artifacts. Intravenous gadolinium contrast was administered when clinically indicated, particularly for evaluation of soft-tissue masses, synovitis, inflammatory pathology, and suspected infective or hypervascular lesions.

MRI images were systematically reviewed for traumatic abnormalities involving the osseous and soft-tissue structures of the wrist. The assessed findings included fractures, bone marrow edema, ligamentous injuries, tendon injuries, triangular fibrocartilage complex (TFCC) abnormalities, joint effusion, synovial abnormalities, and other intra-articular or extra-articular injuries.

For the purpose of the study, a combined wrist injury was defined as the presence of two or more distinct traumatic abnormalities involving different anatomical structures on the same MRI examination. Combined injury patterns were categorized according to the structures involved, including osseous, ligamentous, tendinous, TFCC, and other soft-tissue injuries. The frequency of individual injuries and the distribution of different combinations were recorded.

Correlation With Surgical and Other Findings

Where available, intra-operative, histopathological, or FNAC findings were documented and correlated with the corresponding MRI findings. The final diagnosis was established by integrating the available clinical, imaging, pathological, and surgical findings. Such correlation was performed wherever applicable and was not mandatory for inclusion in the study.

Outcome Measures

The primary outcomes were the frequency of combined traumatic wrist injuries detected on MRI and the distribution of different injury patterns according to the anatomical structures involved. Secondary outcomes included the demographic and clinical profile of patients, frequency of individual traumatic abnormalities, mechanism of injury, and correlation of MRI findings with available intra-operative, histopathological, or FNAC findings.

Statistical Analysis

Data were entered into a structured master chart and analyzed using R statistical software. Continuous variables were expressed as mean ± standard deviation for normally distributed data, while categorical variables were presented as frequencies and percentages. The frequency and distribution of individual traumatic abnormalities and combined injury patterns were analyzed using descriptive statistics. Associations between categorical variables were assessed using the Chi-square test or Fisher's exact test, as appropriate. Where a suitable reference diagnosis was available, diagnostic parameters such as sensitivity and specificity were calculated. A p-value <0.05 was considered statistically significant. Results were presented using tables, cross-tabulations, graphs, and descriptive summaries.

RESULTS

A total of **25 patients** were included in the analysis. The demographic, clinical, MRI, and available histopathological/intraoperative findings were evaluated to determine the spectrum and patterns of wrist abnormalities detected on MRI.

Demographic and Clinical Characteristics: The study population comprised 15 males (60.0%) and 10 females (40.0%). Participants were distributed across three age categories, with 9 patients (36.0%) each in the 30–45 years and >45 years groups, while 7 patients (28.0%) were aged 17–30 years. Thus, 72.0% of the study population was aged >30 years.

Wrist pain was the predominant presenting complaint, occurring in 13 patients (52.0%), followed by wrist pain with swelling in 4 patients (16.0%). Radial-sided wrist pain and wrist pain associated with deformity, instability, or restricted movement were each observed in 3 patients (12.0%). Two patients (8.0%) presented with wrist swelling, lump, or mass. [Table 1]

Table 1. Demographic, clinical characteristics, history of trauma, and clinical diagnosis of the study population

Domain	Parameter/category	Frequency (n)	Percentage (%)
Age group	17–30 years	7	28.0
	30–45 years	9	36.0
	>45 years	9	36.0
Sex	Male	15	60.0
	Female	10	40.0
Presenting complaint	Wrist pain, general/non-specific	13	52.0
	Wrist pain with swelling	4	16.0
	Radial-sided wrist pain	3	12.0
	Wrist pain with deformity/instability/restricted movement	3	12.0
	Wrist swelling/lump/mass	2	8.0
History of trauma	Absent	15	60.0
	Present	9	36.0
	Present, old	1	4.0

Clinical diagnosis	Scaphoid fracture	6	24.0
	TFCC tear	4	16.0
	Infective arthritis	3	12.0
	Ganglion cyst	3	12.0
	Scaphoid AVN	2	8.0
	De Quervain tenosynovitis	1	4.0
	Lunate dislocation	1	4.0
	ECU tenosynovitis	1	4.0
	Madelung deformity	1	4.0
	Kienböck disease	1	4.0
	GCT of tendon sheath	1	4.0
	Carpal tunnel syndrome	1	4.0
Total		**25**	**100.0**

MRI Findings and Scaphoid-Related Abnormalities: Scaphoid fracture was the most frequent MRI abnormality, identified in 6 patients (24.0%), followed by TFCC tear in 4 patients (16.0%). Ganglion cyst and infectious arthritis were each identified in 3 patients (12.0%), while scaphoid AVN was observed in 2 patients (8.0%). The remaining MRI abnormalities, including carpal tunnel syndrome, De Quervain tenosynovitis, ECU tenosynovitis, GCT of tendon sheath, Kienböck disease, lunate dislocation, and Madelung deformity, were each identified in 1 patient (4.0%). Among the 6 patients with scaphoid fracture, Herbert type B1 was the most common pattern, accounting for 3 cases (50.0%), followed by B2 in 2 cases (33.3%) and A2 in 1 case (16.7%). The scaphoid waist was the predominant fracture site (83.3%), and articular surface involvement was present in 4 cases (66.7%). Most fractures were undisplaced (66.7%). An associated scapholunate interval widening was identified in 1 case (16.7%). Among the 2 patients with scaphoid AVN, diffuse and proximal-pole patterns were equally represented (50.0% each), with fragmentation and secondary osteoarthritis present in both cases. **[Table 2]**

Table 2. Distribution of MRI Findings and Detailed Characteristics of Scaphoid-Related Abnormalities

Domain	Parameter	Category	Frequency (n)	Percentage (%)
MRI category		Scaphoid fracture	6	24.0
		TFCC tear	4	16.0
		Ganglion cyst	3	12.0
		Infectious arthritis	3	12.0
		Scaphoid AVN	2	8.0
		Carpal tunnel syndrome	1	4.0
		De Quervain tenosynovitis	1	4.0
		ECU tenosynovitis	1	4.0
		GCT of tendon sheath	1	4.0
		Kienböck disease	1	4.0
		Lunate dislocation	1	4.0
		Madelung deformity	1	4.0
Scaphoid fracture (n=6)	**Herbert classification**	A2	1	16.7
		B1	3	50.0
		B2	2	33.3
	Fracture location	Waist	5	83.3
		Proximal pole	1	16.7
		Distal pole	0	0.0
	Articular surface involvement	Present	4	66.7
		Absent	2	33.3
	Displacement	Undisplaced	4	66.7
		Displaced	2	33.3
	Associated injury	None	5	83.3
		Scapholunate interval widening	1	16.7
	AVN in fracture cases	Absent	6	100.0
		Present	0	0.0
Scaphoid AVN (n=2)	**AVN pattern**	Diffuse	1	50.0
		Proximal pole	1	50.0

	Fragmentation	Present	2	100.0
	Associated fracture non-union	Absent	2	100.0
	Secondary osteoarthritis	Present	2	100.0

MRI Characteristics of TFCC Tears, Infectious Arthritis, and Ganglion Cysts: Among the 4 patients with TFCC tears, central tears were predominant (75.0%), and degenerative tears accounted for 75.0% of cases. Palmer types 1B, 2A, 2B, and 2C were equally represented, with 1 case (25.0%) of each type. DRUJ instability was present in 1 patient (25.0%), while neutral and positive ulnar variance were each observed in 2 cases (50.0%). Among the 3 patients with infectious arthritis, monoarticular involvement was more frequent (66.7%) than polyarticular involvement (33.3%). Synovial thickening was present in all cases, bone marrow edema in 2 cases (66.7%), and adjacent osteomyelitis or abscess in 1 case (33.3%). All 3 ganglion cysts were dorsal and uniloculated, with radiocarpal location being most common (66.7%). None demonstrated adjacent tendon compression. **[Table 3]**

Table 3. Detailed MRI Characteristics of TFCC Tears, Infectious Arthritis, and Ganglion Cysts

Domain	Parameter	Category	Frequency (n)	Percentage (%)
TFCC tear (n=4)	**Palmer classification**	Type 1B	1	25.0
		Type 2A	1	25.0
		Type 2B	1	25.0
		Type 2C	1	25.0
	DRUJ instability	Present	1	25.0
		Absent	3	75.0
	Tear location	Central	3	75.0
		Peripheral	1	25.0
	Tear type	Degenerative	3	75.0
		Traumatic	1	25.0
	Ulnar variance	Neutral	2	50.0
		Positive	2	50.0
		Negative	0	0.0
Infectious arthritis (n=3)	**Joint involvement**	Monoarticular	2	66.7
		Polyarticular	1	33.3
	Joint effusion grade	Mild	1	33.3
		Moderate	1	33.3
		Severe	1	33.3
	Synovial thickening	Present	3	100.0
	Adjacent osteomyelitis/abscess	Present	1	33.3
		Absent	2	66.7
	Bone marrow edema	Present	2	66.7
		Absent	1	33.3
Ganglion cyst (n=3)	**Type**	Dorsal	3	100.0
		Volar	0	0.0
	Location	Radiocarpal	2	66.7
		Intercarpal	1	33.3
		TFCC-related	0	0.0
	Loculation	Uniloculated	3	100.0
		Multiloculated	0	0.0
	Adjacent tendon compression	Present	0	0.0
		Absent	3	100.0

Diagnostic Performance of MRI for Various Wrist Pathologies Using Histopathology/Intraoperative Findings as Reference Standard: MRI demonstrated excellent diagnostic performance across the evaluated wrist pathologies when compared with the available histopathological/intraoperative reference findings. Sensitivity, specificity, PPV, NPV, accuracy, Kappa coefficient, and AUC were 1.00 for most conditions, indicating complete diagnostic agreement between MRI and the reference diagnosis.

The diagnostic performance was also perfect for scaphoid fracture, TFCC tear, scaphoid AVN, infectious arthritis, Kienböck disease, lunate dislocation, Madelung deformity, GCT of tendon sheath, carpal tunnel syndrome, De Quervain tenosynovitis, and ECU tenosynovitis, with no false-positive or false-negative cases reported. For example, MRI correctly identified all 6 scaphoid fractures and all 4 TFCC tears, with sensitivity, specificity, PPV, NPV, accuracy, Kappa, and AUC of 1.00.

Ganglion cyst was the only pathology showing slightly reduced diagnostic performance, with sensitivity and NPV of 1.00, but specificity of 0.96, PPV of 0.67, accuracy of 0.96, Kappa of 0.78, and AUC of 0.98. This was attributable to one MRI-diagnosed ganglion cyst that was classified as a synovial cyst on the reference assessment. Overall, these findings indicate that MRI provided highly reliable characterization of wrist pathology in the present study, with near-perfect agreement with the available histopathological/intraoperative findings. [Table 4]

Table 4: Diagnostic Performance of MRI for Various Wrist Pathologies Using Histopathology/Intraoperative Findings as Reference Standard

Disease	TP	FP	TN	FN	Sensitivity	Specificity	PPV	NPV	Accuracy	Kappa	AUC
Carpal tunnel syndrome	1	0	24	0	1.00	1.00	1.00	1.00	1.00	1.00	1.00
De Quervain tenosynovitis	1	0	24	0	1.00	1.00	1.00	1.00	1.00	1.00	1.00
ECU tenosynovitis	1	0	24	0	1.00	1.00	1.00	1.00	1.00	1.00	1.00
Ganglion cyst	2	1	22	0	1.00	0.96	0.67	1.00	0.96	0.78	0.98
GCT of tendon sheath	1	0	24	0	1.00	1.00	1.00	1.00	1.00	1.00	1.00
Infectious arthritis	3	0	22	0	1.00	1.00	1.00	1.00	1.00	1.00	1.00
Kienböck disease	1	0	24	0	1.00	1.00	1.00	1.00	1.00	1.00	1.00
Lunate dislocation	1	0	24	0	1.00	1.00	1.00	1.00	1.00	1.00	1.00
Madelung deformity	1	0	24	0	1.00	1.00	1.00	1.00	1.00	1.00	1.00
Scaphoid AVN	2	0	23	0	1.00	1.00	1.00	1.00	1.00	1.00	1.00
Scaphoid fracture	6	0	19	0	1.00	1.00	1.00	1.00	1.00	1.00	1.00
TFCC tear	4	0	21	0	1.00	1.00	1.00	1.00	1.00	1.00	1.00

Distribution of Histopathology/intra op findings Category: Histopathology/intra op findings category showed that scaphoid fracture was the most common finding, observed in 6 cases and accounting for 24% of the total study population. TFCC tear was present in 4 cases (16%), while infectious arthritis was noted in 3 cases (12%). Ganglion cyst and Scaphoid AVN were observed in 2 cases each, representing 8% each. The remaining categories, including Carpal tunnel syndrome, De Quervain tenosynovitis, ECU tenosynovitis, GCT of tendon sheath, Kienbock disease, Lunate dislocation, Madelung deformity, and Synovial cyst, were each seen in 1 case (4%). [Table 5]

Table 5: Distribution of histopathology/intra op findings category

Histopathology/intra op findings category	Frequency (n)	Percentage (%)
Carpal tunnel syndrome	1	4
De Quervain tenosynovitis	1	4
ECU tenosynovitis	1	4
Ganglion cyst	2	8
GCT of tendon sheath	1	4
Infectious arthritis	3	12
Kienbock disease	1	4
Lunate dislocation	1	4
Madelung Deformity	1	4
Scaphoid AVN	2	8
Scaphoid fracture	6	24
Synovial cyst	1	4
TFCC tear	4	16
Total	25	100

Correlation Between MRI Diagnosis and Histopathological/Intraoperative Findings: MRI showed excellent correlation with the available histopathological/intraoperative findings, with concordant diagnoses in 24 of 25 patients (96.0%). Complete agreement was observed for all evaluated pathologies except ganglion cyst. Of the three cases diagnosed as ganglion cyst on MRI, two (8.0%) were confirmed as ganglion cysts, while one (4.0%) was reported as a synovial cyst on the reference assessment. Thus, only one discordant case (4.0%) was observed, indicating a high level of diagnostic concordance between MRI and the reference findings.

Table 6. Correlation Between MRI Diagnosis and Histopathological/Intraoperative Findings

MRI diagnosis	Histopathological/Intraoperative diagnosis	n (%)	Agreement
Carpal tunnel syndrome	Carpal tunnel syndrome	1 (4.0)	Concordant
De Quervain tenosynovitis	De Quervain tenosynovitis	1 (4.0)	Concordant
ECU tenosynovitis	ECU tenosynovitis	1 (4.0)	Concordant
Ganglion cyst	Ganglion cyst	2 (8.0)	Concordant
Ganglion cyst	Synovial cyst	1 (4.0)	Discordant
GCT of tendon sheath	GCT of tendon sheath	1 (4.0)	Concordant
Infectious arthritis	Infectious arthritis	3 (12.0)	Concordant
Kienböck disease	Kienböck disease	1 (4.0)	Concordant
Lunate dislocation	Lunate dislocation	1 (4.0)	Concordant
Madelung deformity	Madelung deformity	1 (4.0)	Concordant
Scaphoid AVN	Scaphoid AVN	2 (8.0)	Concordant
Scaphoid fracture	Scaphoid fracture	6 (24.0)	Concordant
TFCC tear	TFCC tear	4 (16.0)	Concordant
Total		**25 (100.0)**	
Overall concordance		**24 (96.0)**	
Overall discordance		**1 (4.0)**	

Figure 1: Coronal T1 weighted image shows a growth disturbance of the distal radius with the ulnar side of the epiphysis (red arrow) underdeveloped compared to the radial side (blue arrow). On Coronal T2 weighted image an anomalous volar ligament (yellow arrows) originates proximal to the distal radial growth plate and extends to the triquetrum (T). The Axial T1 weighted images show the radial origin of the anomalous ligament (black arrow). Note the mild dorsal subluxation of the ulnar head (U) relative to the distal radius (R). These findings are consistent with Madelung deformity.

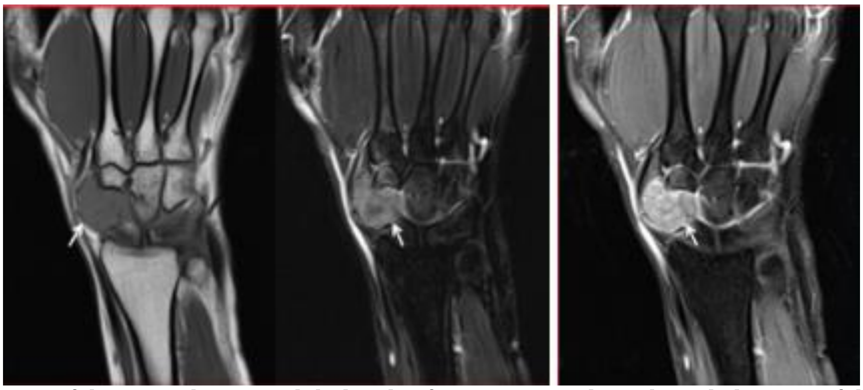

Figure 2: Coronal image of the wrist showing a lobulated soft-tissue mass along the radial aspect of the wrist (arrow). The lesion appears hypointense on T1-weighted imaging, demonstrates heterogeneous hyperintensity on T2 image and shows avid heterogeneous enhancement on post-contrast fat-suppressed T1-weighted images, consistent with a Giant cell tumor of tendon sheath.

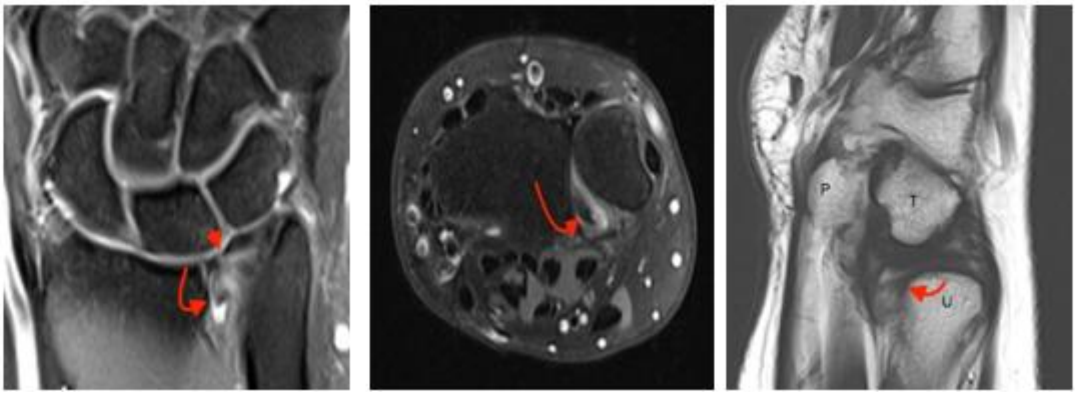

Figure 3: Coronal PD fat suppressed weighted image demonstrates a full thickness tear within the central triangular fibrocartilage (small arrow). A displaced flapped (curved arrow) extends toward the distal radioulnar joint. Axial PD fat suppressed weighted image demonstrates the displaced flap (arrow) located within the volar aspect of the distal radioulnar joint. Sagittal T2 weighted image at level of the pisiform (P) and Triquetrum (T) again demonstrates the displaced triangular fibrocartilage flap (arrow) along the volar aspect of the distal ulna (U). Findings consistent with Full-thickness central TFCC tear.

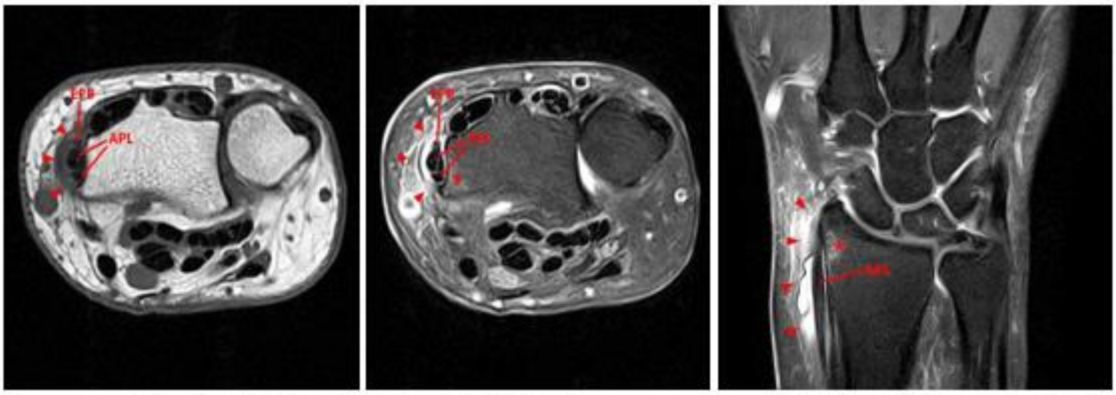

Figure 4: The Axial T1-weighted, Axial PD fat-suppressed weighted, and Coronal PD fat-suppressed weighted images demonstrate a thickened extensor retinaculum, surrounding soft tissue edema, and fluid signal in the first extensor compartment of the wrist (arrowheads). Marrow edema is noted within the subjacent radius (asterisks). A single extensor pollicis brevis and two abductor pollicis longus tendon slips are present with heterogeneous intrinsic signal. These findings are consistent with De Quervain's tenosynovitis.

Figure 5: Coronal T1-weighted image demonstrates diffuse hypointense marrow signal within the lunate bone with loss of normal fatty marrow signal, consistent with Kienböck disease (avascular necrosis of the lunate).

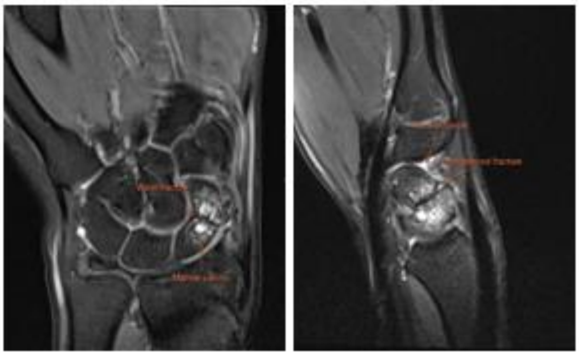

Figure 6: Coronal PD fat-suppressed image shows a fracture through the waist of the scaphoid with marrow edema evident as hyperintense signal intensity surrounding the fracture site. Sagittal PD fat-suppressed image demonstrates an undisplaced scaphoid waist fracture with associated bone marrow and a small joint effusion. These findings support the diagnosis of an acute Scaphoid waist fracture.

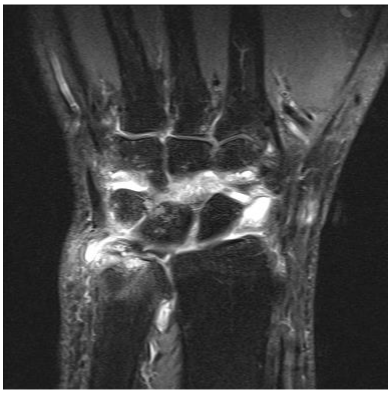

Figure 7: Coronal PD fat-suppressed image showing marked fluid signal within the radiocarpal and intercarpal joints, consistent with a wrist joint effusion and adjacent marrow edema. Synovial thickening and hyperintense signal surrounding the carpal bones and within the soft tissues adjacent to the wrist, indicating inflammatory change and associated edema. Findings suggesting Infectious arthritis.

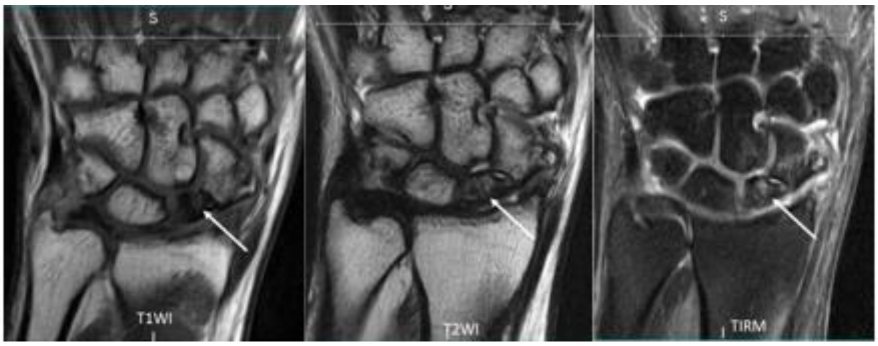

Figure 8: Coronal T1-weighted image (left) shows diffuse low signal intensity within the proximal pole of the scaphoid (arrow). Coronal T2-weighted image (middle) demonstrates persistent low signal intensity (arrow). Coronal TIRM image (right) shows surrounding marrow edema with altered signal intensity in the proximal pole (arrow). Findings consistent with Avascular necrosis of scaphoid at proximal pole.

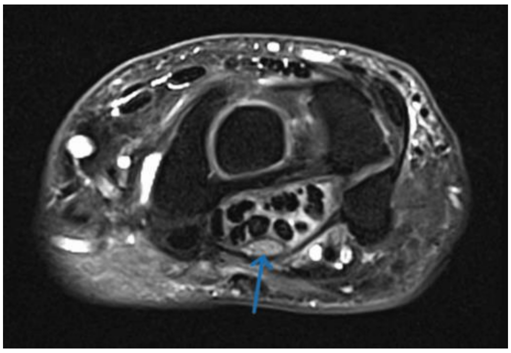

Figure 9: Axial T2-weighted fat-suppressed image shows median nerve (arrow) within the carpal tunnel is enlarged and shows increased T2 signal intensity, consistent with neural edema secondary to compressive neuropathy.

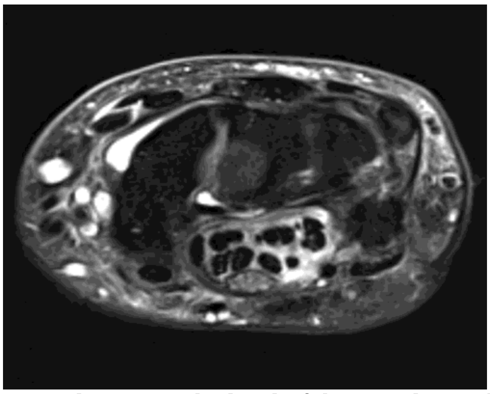

Figure 10: Axial T2-weighted fat-suppressed image at the level of the carpal tunnel showing fluid surrounding the flexor tendons, indicative of flexor tenosynovitis. The resultant increase in tunnel contents leading to median nerve compression. These findings are suggestive of Carpal tunnel syndrome.

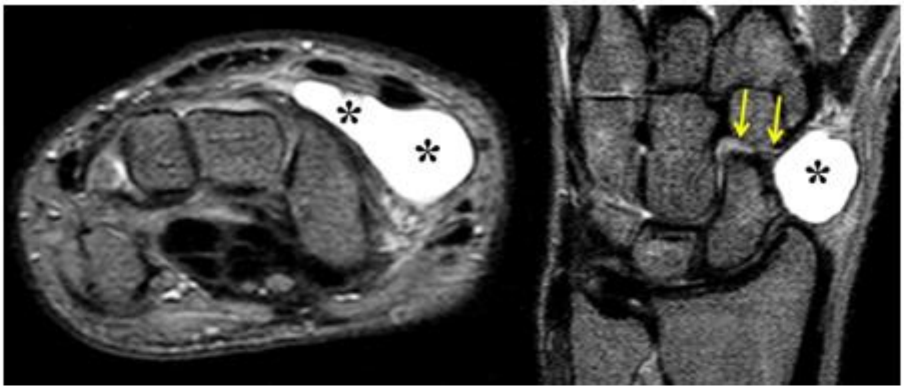

Figure 11: Axial and Coronal T2-weighted fat-suppressed MRI shows a well-defined, hyperintense cystic structure (asterisk) along the dorsal aspect of the wrist with a communicating stalk/pedicle (arrows) arising from the scaphotrapeziotrapezoid joint. The marked hyperintensity indicates fluid content. Findings consistent with Ganglion cyst.

DISCUSSION

The present study evaluated 25 patients with wrist pain using MRI and demonstrated a broad spectrum of osseous, ligamentous, fibrocartilaginous, inflammatory, cystic, tendon-related, and nerve-related abnormalities. Most patients were older than 30 years, and males constituted 60.0% of the cohort. Generalized or non-specific wrist pain was the commonest presentation (52.0%), while a history of trauma was absent in 60.0% of patients. This heterogeneous presentation highlights the difficulty of establishing a definitive diagnosis on clinical assessment alone and supports the role of MRI as a problem-solving modality. Similar observations were reported by Huellner et al., who emphasized the usefulness of MRI for lesion localization and characterization of soft-tissue and ligamentous abnormalities in patients with chronic hand or wrist pain [15]. The present findings also support the observations of El-Kholy et al., who demonstrated that MRI can reveal a wide range of osseous and soft-tissue abnormalities in patients with painful wrists [16].

Scaphoid fracture was the most frequent MRI diagnosis, occurring in 6 patients (24.0%). Among these, five fractures (83.3%) involved the waist and one (16.7%) involved the proximal pole. Herbert type B1 was most common (50.0%), followed by B2 (33.3%) and A2 (16.7%). Articular surface involvement was present in 66.7% and displacement in 33.3%. One patient (16.7%) showed scapholunate interval widening. These findings demonstrate that MRI provides information beyond simple fracture detection by defining fracture location, morphology, displacement, articular involvement, and associated ligamentous abnormalities. Huellner et al. similarly emphasized the value of MRI in lesion detection and localization [15]. Matthews et al. recommended a structured approach to wrist MRI that includes assessment of osseous, ligamentous, cartilage, and tendon abnormalities, which is particularly relevant in scaphoid injuries where associated instability may influence management [17].

TFCC tear was the second most frequent abnormality, accounting for 16.0% of cases. Central tears predominated (75.0%), and degenerative tears were more common than traumatic tears (75.0% vs. 25.0%). Positive ulnar variance was present in half of the cases, while DRUJ instability was identified in one patient. These findings suggest that many TFCC lesions in the present cohort had a degenerative or loading-related component rather than being purely traumatic. Boer et al., in a larger cohort of 150 patients, reported that MR arthrography was slightly more accurate than conventional MRI for TFCC lesions, although conventional MRI remained reliable [18]. Omar et al. similarly found that MR arthrography detected more subtle TFCC and ligamentous lesions, while conventional MRI performed comparably for tendon and osseous abnormalities [19]. In the present study, conventional MRI showed complete diagnostic concordance for TFCC tears, with sensitivity, specificity, PPV, NPV, accuracy, Kappa, and AUC all equal to 1.00. The excellent performance may reflect the clinically significant nature of the tears included in this relatively small cohort.

Infectious arthritis was identified in 3 patients (12.0%). Synovial thickening was present in all cases, bone marrow edema in 66.7%, and adjacent osteomyelitis or abscess in 33.3%. MRI therefore demonstrated not only the intra-articular abnormality but also marrow and periarticular extension. Although Glinatsi et al. evaluated rheumatoid rather than infectious arthritis, their findings showed that MRI-detected synovitis, tenosynovitis, and osteitis are associated with pain and functional impairment [20]. Gornitzky et al. also emphasized the selective usefulness of wrist MRI in suspected infection, masses, and arthropathies [21]. In the present study, infectious arthritis showed complete diagnostic agreement with the available reference findings, further supporting the value of MRI in clinically suspected inflammatory or infective wrist disease.

Scaphoid AVN was identified in 2 patients (8.0%), with one diffuse and one proximal-pole pattern. Both cases demonstrated fragmentation and secondary osteoarthritis. Kienböck disease was identified in one additional patient. These findings emphasize the ability of MRI to detect vascular and structural abnormalities of the carpal bones and to demonstrate associated degenerative changes. El-Kholy et al. reported AVN as the most frequent non-traumatic MRI abnormality in their cohort [16]. In contrast, scaphoid fracture was the dominant finding in the present study, probably reflecting differences in referral patterns and the proportion of trauma-related cases. Nevertheless, both studies support MRI as an important modality for evaluating osteonecrotic and degenerative wrist pathology.

Ganglion cysts were detected in 3 patients (12.0%), all of which were dorsal and uniloculated. Two were radiocarpal and one was intercarpal. GCT of tendon sheath was identified in one patient. Couzens et al. demonstrated that ganglion cysts and other MRI abnormalities can also occur in asymptomatic wrists, emphasizing the importance of clinical correlation [22]. This issue was evident in the present study because two MRI-diagnosed ganglion cysts were confirmed as ganglion cysts, whereas one was classified as a synovial cyst on histopathological/intra-operative assessment. Consequently, ganglion cyst had slightly lower diagnostic performance, with accuracy of 96.0% and Kappa of 0.78, despite sensitivity and NPV of 100%. This suggests that MRI is highly sensitive for identifying cystic lesions but that exact characterization may occasionally require pathological or operative confirmation.

The study also demonstrated several less common but clinically relevant abnormalities, including De Quervain tenosynovitis, ECU tenosynovitis, carpal tunnel syndrome, lunate dislocation, Madelung deformity, Kienböck disease, and GCT of tendon sheath. Although each accounted for only 4.0% of cases, their identification illustrates the advantage of evaluating the wrist systematically rather than focusing exclusively on the suspected clinical diagnosis. El-Leithy reported that MRI was particularly useful for deep structures, marrow abnormalities, ligament tears, and instability, while ultrasonography had advantages for superficial tendon pathology [23]. Similarly, Al-Aswad et al. demonstrated the usefulness of MRI across traumatic, inflammatory, degenerative, and tendon-related wrist disorders [24].

Overall, MRI demonstrated excellent correlation with histopathological/intra-operative findings. Complete diagnostic agreement was observed for scaphoid fracture, TFCC tear, infectious arthritis, scaphoid AVN, GCT of tendon sheath, tendon disorders, carpal tunnel syndrome, Kienböck disease, lunate dislocation, and Madelung deformity. The only discordance occurred with a cystic lesion. These results are consistent with the findings of Götestrand et al., who reported that standard 3-Tesla MRI provides clinically adequate diagnostic performance for wrist ligamentous pathology [25]. However, the very high diagnostic values in the present study should be interpreted cautiously because of the small sample size of 25 patients and the limited number of cases within individual diagnostic categories.

Despite these findings, the present study had certain limitations, including its relatively small sample size and single-centre design, which may limit generalizability. The small number of patients in individual diagnostic categories restricted subgroup analysis. Histopathological or intra-operative correlation was available only in selected cases, while long-term outcomes and interobserver variability were not assessed.

Taken together, the findings indicate that MRI provides comprehensive evaluation of wrist pain by simultaneously assessing bone, marrow, ligaments, TFCC, tendons, synovium, cystic lesions, and surrounding soft tissues. The broad spectrum of abnormalities despite predominantly non-specific clinical presentations supports its role as a problem-solving investigation. Nevertheless, MRI findings should always be interpreted in conjunction with clinical information and, where available, operative or histopathological findings, particularly for lesions with overlapping imaging appearances.

CONCLUSION

MRI was highly effective in evaluating wrist pain, identifying a broad spectrum of osseous, ligamentous, inflammatory, cystic, tendon, and nerve-related abnormalities. Scaphoid fracture was the most common finding (24.0%), followed by TFCC tear (16.0%). MRI provided detailed lesion characterization and showed excellent diagnostic concordance with histopathological/intra-operative findings, with most parameters demonstrating 100% diagnostic performance. The only discrepancy involved one ganglion cyst classified as a synovial cyst. Overall, MRI represents a comprehensive and reliable modality for clinically selected patients with traumatic, persistent, or non-specific wrist symptoms, although findings should be correlated with clinical and pathological evidence when available.

REFERENCES

1. Vassa R, Garg A, Omar IM. Magnetic resonance imaging of the wrist and hand. Pol J Radiol. 2020 Aug 26;85:e461-e488. doi: 10.5114/pjr.2020.99034.
2. ReghunAth A, Singh DK, AggARwAl A, BABBAR N, CHOUDHARY R, SURYA S. MRI and MR Arthrography Imaging of the Pathologies of the Wrist: A Pictorial Essay. Journal of Clinical & Diagnostic Research. 2022 Dec 1;16(12).
3. Sedeek FR, Othman MH, Mohammad AH. Role of MRI in evaluation of wrist ligament injury. Journal of Current Medical Research and Practice. 2020 Apr 1;5(2):180-4.
4. ReghunAth A, Singh DK, AggARwAl A, BABBAR N, CHOUDHARY R, SURYA S. MRI and MR Arthrography Imaging of the Pathologies of the Wrist: A Pictorial Essay. Journal of Clinical & Diagnostic Research. 2022 Dec 1;16(12).
5. Morris CJ, Younan Y, Singer AD, Johnson G, Chamieh J, Datir A. Masses of the hand and wrist, a pictorial review. Clin Imaging. 2016 Jul-Aug;40(4):650-65. doi: 10.1016/j.clinimag.2016.02.019. Epub 2016 Feb 23.
6. Howe BM, Spinner RJ, Felmlee JP, Frick MA. MR Imaging of the Nerves of the Upper Extremity: Elbow to Wrist. Magn Reson Imaging Clin N Am. 2015 Aug;23(3):469-78. doi: 10.1016/j.mric.2015.04.009.
7. El-Deek AM, Dawood EM, Mohammed AA. Role of ultrasound versus magnetic resonance imaging in evaluation of non-osseous disorders causing wrist pain. Egyptian Journal of Radiology and Nuclear Medicine. 2019 Sep 2;50(1):8.
8. Hampole AB, Jeevika MU, Nirnay KK, Hita S, Anup S, Ganesh G. Ultrasonography and MRI evaluation in wrist joint pain. Asian J Med Radiol Res. 2021 Jan;9(1):17.
9. Johnson D, Stevens KJ, Riley G, Shapiro L, Yoshioka H, Gold GE. Approach to MR Imaging of the Elbow and Wrist: Technical Aspects and Innovation. Magn Reson Imaging Clin N Am. 2015 Aug;23(3):355-66. doi: 10.1016/j.mric.2015.04.008. Epub 2015 May 21.
10. Gartner L, Pearce CJ, Saifuddin A. The role of the plain radiograph in the characterisation of soft tissue tumours. Skeletal Radiol. 2009 Jun;38(6):549-58. doi: 10.1007/s00256-008-0513-9. E
11. Nascimento D, Suchard G, Hatem M, de Abreu A. The role of magnetic resonance imaging in the evaluation of bone tumours and tumour-like lesions. Insights Imaging. 2014 Aug;5(4):419-40. doi: 10.1007/s13244-014-0339-z.
12. Hobby JL, Tom BD, Bearcroft PW, Dixon AK. Magnetic resonance imaging of the wrist: diagnostic performance statistics. Clin Radiol. 2001 Jan;56(1):50-7. doi: 10.1053/crad.2000.0571.
13. Torabi M, Martell B, Stubbs AJ, Lenchik L. MRI–Arthroscopy Correlation of the Hip: A Primer for Radiologists. Current radiology reports. 2016 Apr 22;4(6):35.

14. Chun KY, Choi YS, Lee SH, Kim JS, Young KW, Jeong MS, Kim DJ. Deltoid Ligament and Tibiofibular Syndesmosis Injury in Chronic Lateral Ankle Instability: Magnetic Resonance Imaging Evaluation at 3T and Comparison with Arthroscopy. Korean J Radiol. 2015 Sep-Oct;16(5):1096-103. doi: 10.3348/kjr.2015.16.5.1096.
15. Huellner MW, Bürkert A, Strobel K, Pérez Lago Mdel S, Werner L, Hug U, von Wartburg U, Seifert B, Veit-Haibach P. Imaging non-specific wrist pain: interobserver agreement and diagnostic accuracy of SPECT/CT, MRI, CT, bone scan and plain radiographs. PLoS One. 2013 Dec 30;8(12):e85359. doi: 10.1371/journal.pone.0085359.
16. El-Kholy M, Maaly M, Hemeeda Y. Role of MRI in evaluation of painful wrist joint. Menoufia Medical Journal. 2015 Apr 1;28(2):503-.
17. Matthews GS, Kiani B, Wuertzer SD, Powell JA, Roller BL, Lenchik L, Torabi M. MRI of the Wrist: Algorithmic Approach for Evaluating Wrist Pain. Radiographics. 2019 Mar-Apr;39(2):447-448. doi: 10.1148/rg.2019180157.
18. Boer BC, Vestering M, van Raak SM, van Kooten EO, Huis In 't Veld R, Vochteloo AJH. MR arthrography is slightly more accurate than conventional MRI in detecting TFCC lesions of the wrist. Eur J Orthop Surg Traumatol. 2018 Dec;28(8):1549-1553. doi: 10.1007/s00590-018-2215-x.
19. Omar NN, Mahmoud MK, Saleh WR, Almallah HG, Qenawy OK, Mourad AF, Abdul Monem ES. MR arthrography versus conventional MRI and diagnostic arthroscope in patients with chronic wrist pain. Eur J Radiol Open. 2019 Jul 22;6:265-274. doi: 10.1016/j.ejro.2019.06.003.
20. Glinatsi D, Brahe CH, Hetland ML, Ørnbjerg L, Krabbe S, Baker JF, Boesen M, Rastiemadabadi Z, Morsel-Carlsen L, Røgind H, Hansen A, Nørregaard J, Jacobsen S, Terslev L, Huynh TK, Manilo N, Jensen DV, Møller JM, Krogh NS, Østergaard M. Association between MRI findings and patient-reported outcomes in patients with rheumatoid arthritis in clinical remission and at relapse. Int J Rheum Dis. 2020 Apr;23(4):488-498. doi: 10.1111/1756-185X.13790.
21. Gornitzky AL, Lin IC, Carrigan RB. The Diagnostic Utility and Clinical Implications of Wrist MRI in the Pediatric Population. Hand (N Y). 2018 Mar;13(2):143-149. doi: 10.1177/1558944717695752.
22. Couzens G, Daunt N, Crawford R, Ross M. Positive magnetic resonance imaging findings in the asymptomatic wrist. ANZ J Surg. 2014 Jul-Aug;84(7-8):528-32. doi: 10.1111/ans.12552.
23. El-Leithy NE, Kamal H. Ulnar-sided traumatic wrist pain: high-resolution ultrasound effectiveness versus MRI assessment and accuracy. Med J Cairo Univ. 2021;89(6):1051-1061.
24. AbdAl Aziz Al Aswad N, Radwan SA, Esmail MA, El-Saadany HM, Teama AH. Diagnostic and interventional role of magnetic resonance imaging and ultrasound in painful wrist conditions. Egypt J Hosp Med. 2023;90(1):1087-1097.
25. Götestrand S, Flondell M, Lundin B, Aksyuk E, Shalhoub RA, Szaro P, et al. MRI of wrist ligament trauma was similar at 7 T and 3 T with arthroscopy as a reference standard. Eur Radiol. 2025 May 8:1-9.